A：Solar-Cで探る新しい太陽物理学とその広がり

17a

恒星彩層活動の本質を見極める SOLAR-C

渡邊鉄哉（国立天文台）

Contents

- Chromospheres in Solar/Stellar Connection
  - Radiative Energy Losses
  - Chromospheric vs Coronal Heating

- Basal Heating of the Chromosphere
  - Non-magnetic origin vs magnetic activity
- COmosphere
  - Thermal bifurcation
  - Formation height
  - Flows

Solar Energy Losses

Table 1 Chromospheric and coronal energy losses

Parameter	Quiet Sun	Coronal hole	Active region
Transition layer pressure (dyn cm^{-2})	2×10^{-1}	7×10^{-2}	2
Coronal temperature (K, at $r \approx 1.1\ R_\odot$)	1.1 to 1.6×10^6	10^6	2.5×10^6
Coronal energy losses (erg cm^{-2} sec^{-1})			
Conduction flux F_c	2×10^5	6×10^4	10^5 to 10^7
Radiative flux F_r	10^5	10^4	5×10^6
Solar wind flux F_w	$\lesssim 5 \times 10^4$	7×10^5	$(< 10^5)$
Total corona loss $F_c + F_r + F_w$	3×10^5	8×10^5	10^7
Chromospheric radiative losses			
(erg cm^{-2} sec^{-1})[a]			
Low chromosphere	2×10^6	2×10^6	$\gtrsim 10^7$
Middle chromosphere	2×10^6	2×10^6	10^7
Upper chromosphere	3×10^5	3×10^5	2×10^6
Total chromospheric loss	4×10^6	4×10^6	2×10^7
Solar wind mass loss (g cm^{-2} sec^{-1})	$\lesssim 2 \times 10^{-11}$	2×10^{-10}	$(< 4 \times 10^{-11})$

[a] Based on Athay's (1976) estimates for the quiet Sun; see text.

Withbroe & Noyes

(Ann. Rev. Astron. Astrophys., 15, 363, 1977)

Energy Flux out of Stars

$$\nabla(\vec{F}_r + \vec{F}_c + \vec{F}_m + \vec{F}_g + \vec{F}_k + \vec{F}_e) = 0$$

$\vec{F}_r$; radiative $\vec{F}_c$; conductive $\vec{F}_m$; mechanical

$\vec{F}_g$; gravitational $\vec{F}_{\mathrm{k}}$; kinematic $\vec{F}_e$; enthalpy

at $\tau_c \sim 10^{-4}$ (T_{min}), $\Delta T \sim$ 150K

$\Delta H/H \sim 16T^3/T_{eff}^4 \Delta T \tau_c \sim 10^{-3}$ $\Delta T \tau_c \sim 1.5 \times 10^{-5}$

Chromosphere; $(3-6) \times 10^6$ erg/cm^{2}sec

$\rightarrow \Delta H/H \sim (5-8) \times 10^{-5}$ erg/cm^{2}sec

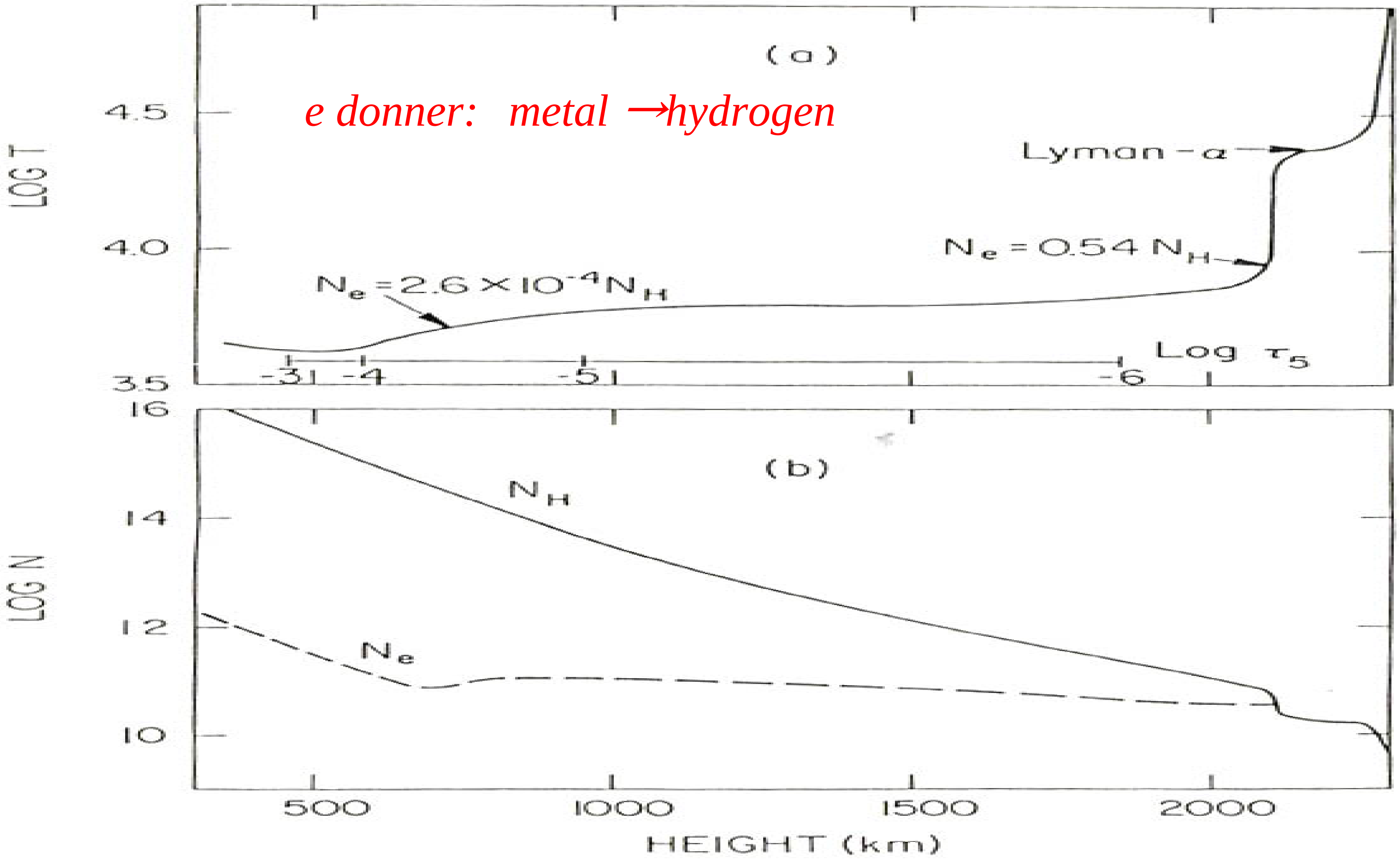

e donner: metal →hydrogen
(a)
(b)
LOG T
LOG N
4.5
4.0
3.5
16
14
12
10
Lyman-α
Ne=0.54 NH
Ne=2.6×10⁻⁴NH
Log τ5
-3
-4
-5
-6
NH
Ne
500
1000
1500
2000
HEIGHT (km)

恒星の磁気活動

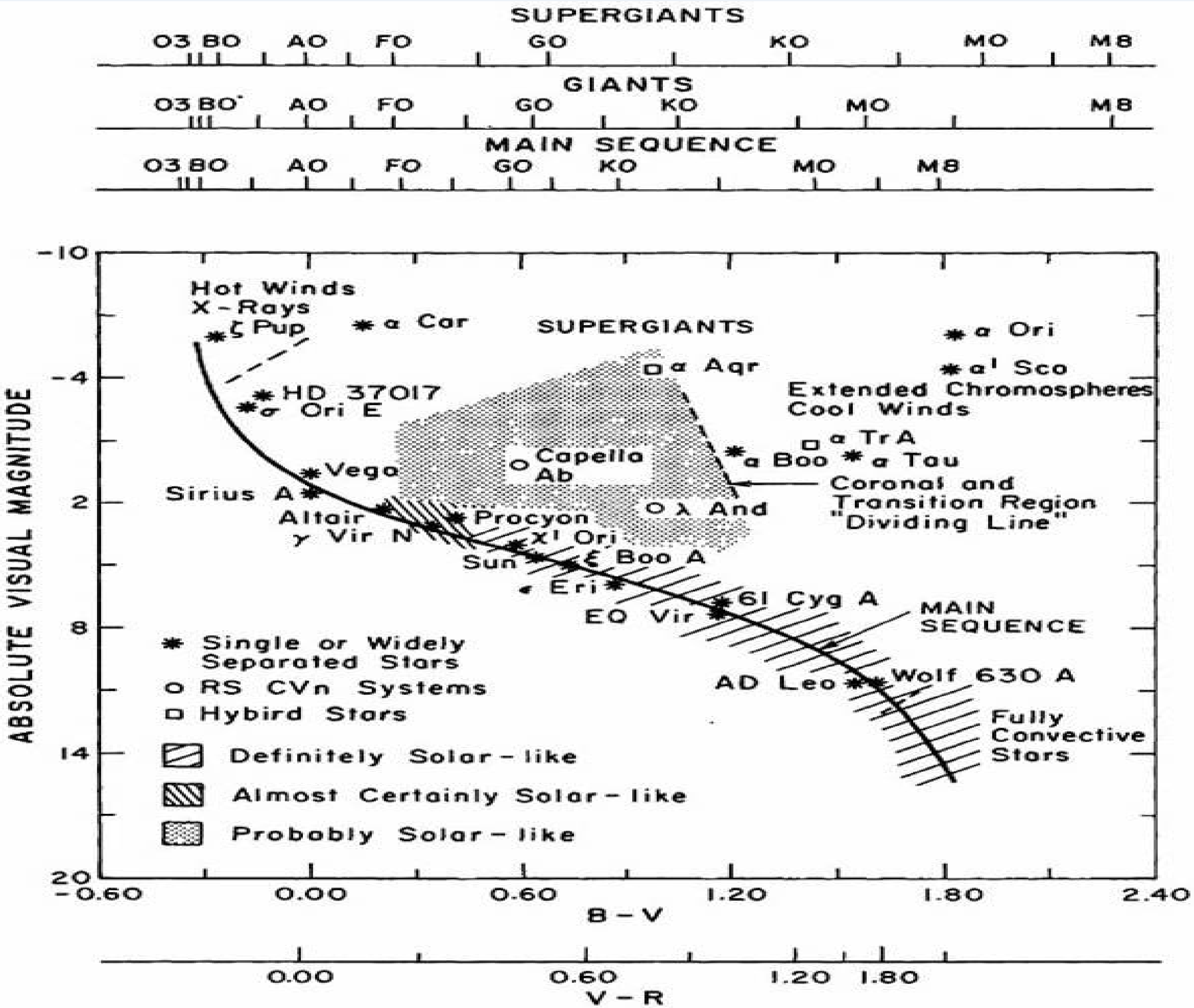

Linsky, SP, 1985, 100, 333

Correlation: Chromosphere vs Corona

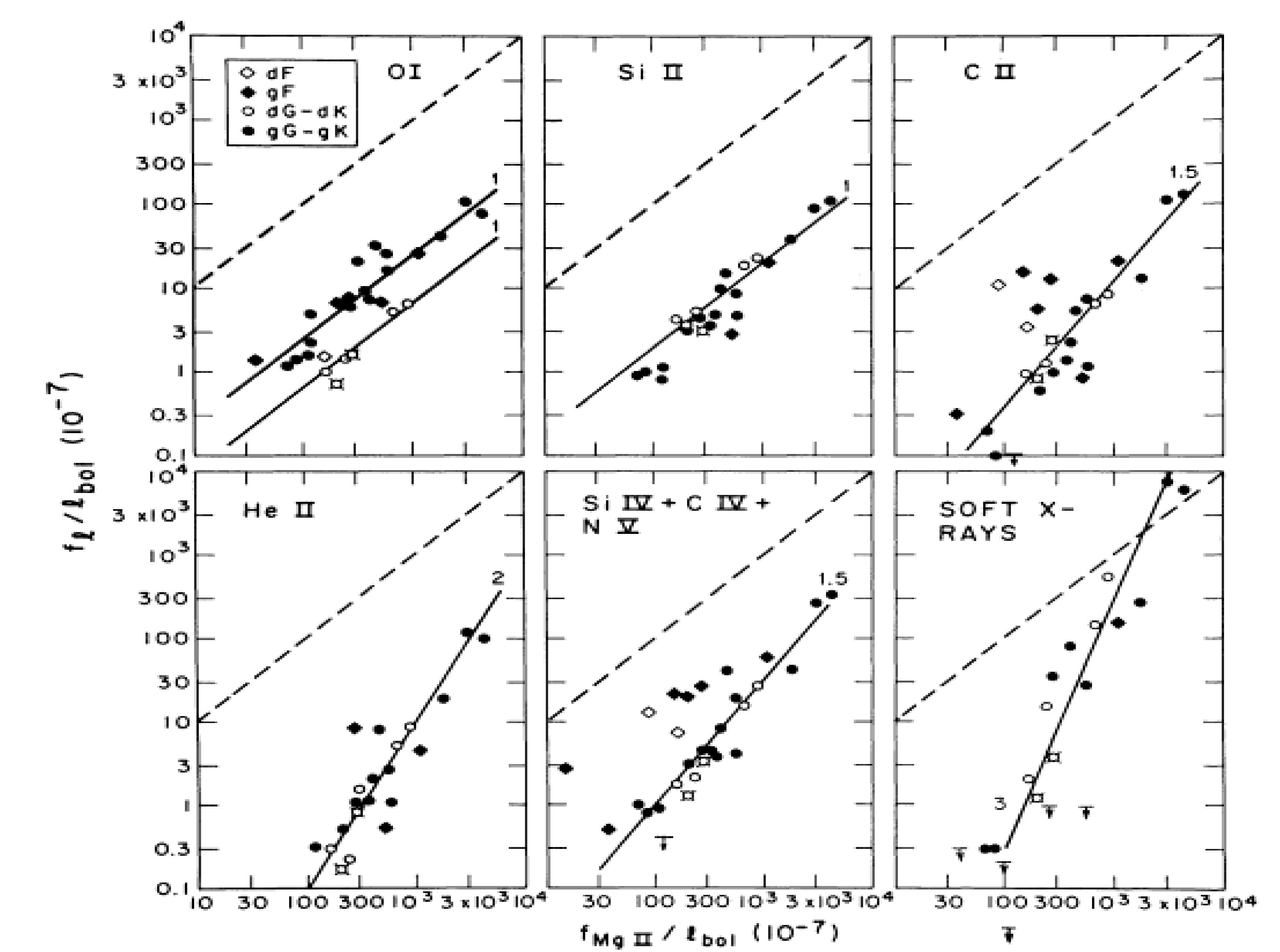

Ayres et al., 1981, ApJ, 247, 545.

Chromospheric Fluxes

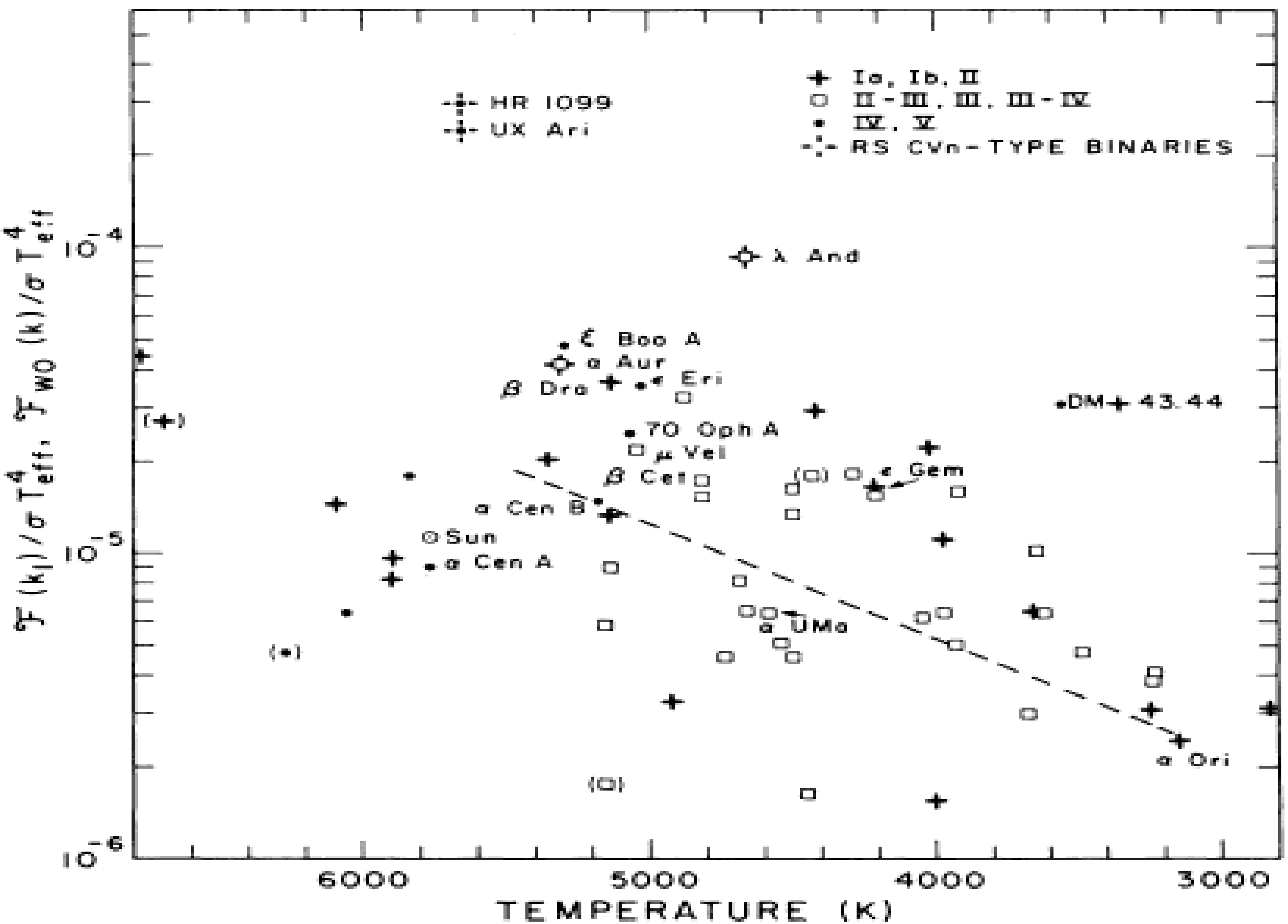

Basri & Linsky 1979 ApJ 234, 1023

Corona – Wind dichotomy

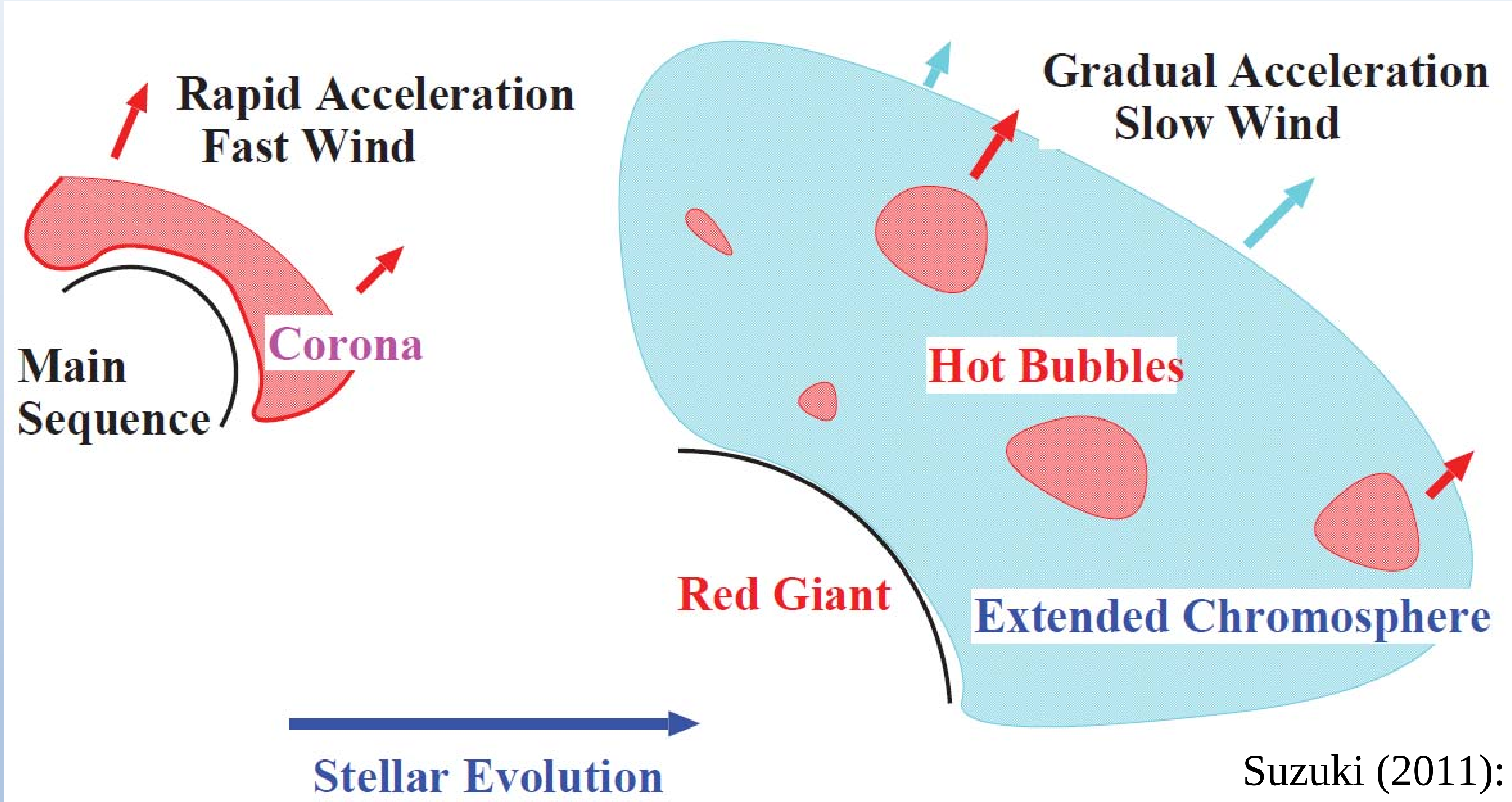

Suzuki (2011):

Basal Chromosphere

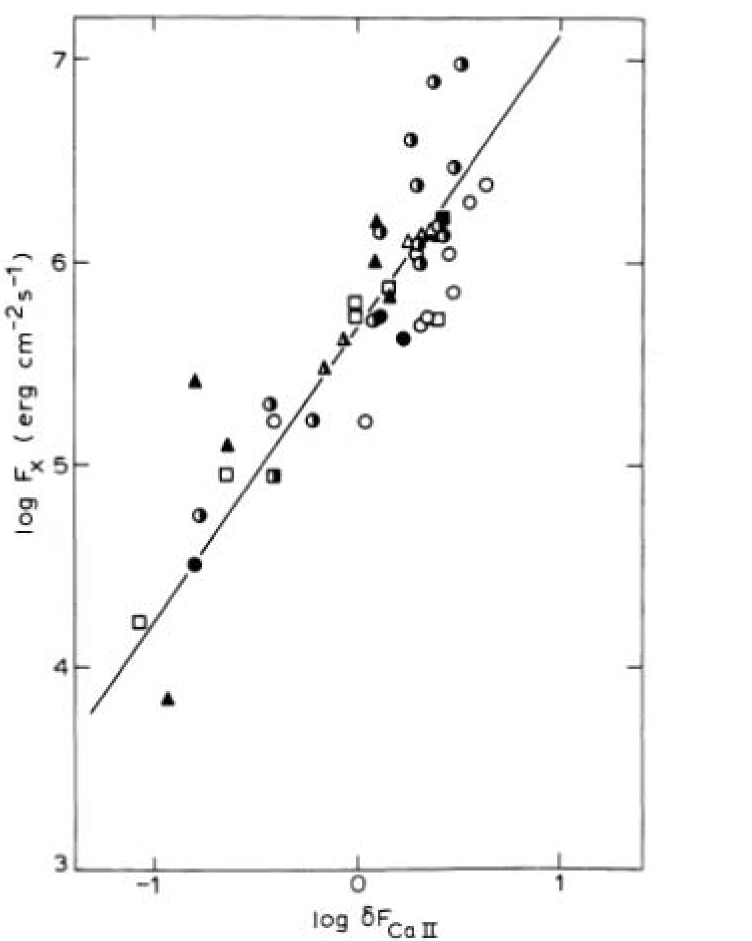

Fig. 3. Soft X-ray flux density F_X versus Ca II H + K excess flux density $\delta F_{Ca\,II} \equiv F_{Ca\,II} - \phi_{Ca\,II}$ using the basal flux density $\phi_{Ca\,II}$ listed in Table 3. Symbols:

LC	II–III/III	III–IV/IV	IV–V/V
$(B-V) < 0.6$	△	□	○
$0.6 \le (B-V) < 0.8$	△	□	◑
$0.8 \le (B-V) < 1.0$	▲	◨	●
$1.0 \le (B-V)$	▲	■	●

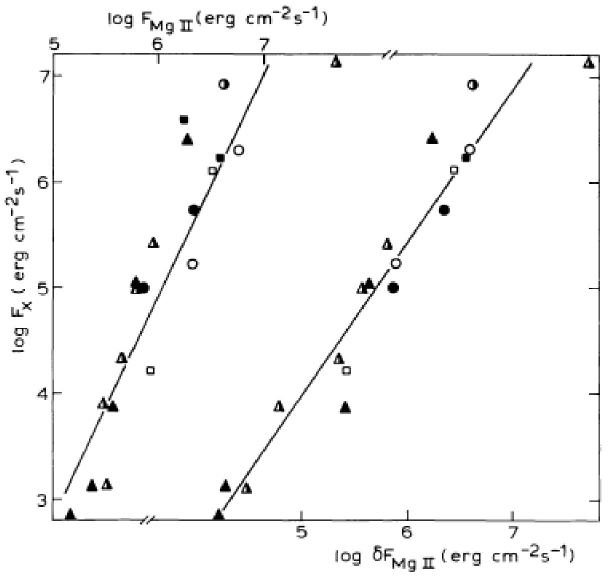

Fig. 5. Soft X-ray flux density F_X against Mg II h + k flux density $F_{Mg\,II}$ (left), and against the excess flux density $\delta F_{Mg\,II} = F_{Mg\,II} - \phi_{Mg\,II}$, $\phi_{Mg\,II}$ as in Table 2. Symbols as in Fig. 3

$F_{ch} = F_{ch\_b} + F_{ch\_a}$

F_{ch_a}: active chromosphere

⇔ coronal activity

← magnetic activity

F_{ch_b} : basal chromosphere

Schrijver (1987)

Table 3. Logarithmic values of the basal flux densities ϕ_i (cf. Eq. 4); $\phi_{Ca\,II}$ is given in relative units, $\phi_{Mg\,II}$ and $\phi_{Si\,II}$ are given in erg cm^{-2} s^{-1}. Uncertain values are put between brackets. Fluxes derived for a sample of giants only are labelled III

		Giants			Dwarfs		
B–V:		0.3	0.48	1.3	0.3	0.48	0.9
Ca II H+K		1.09	0.56	−1.24	1.23	0.48	−0.14
	III	1.11	0.52	−1.25			
Mg II h+k		——	6.19	4.89	——	(6.74	3.06)
	III	——	6.18	4.89			
Si II		——	4.36	3.01	——	——	——

Basal Chromosphere

$$\log (F_i - \phi_i) = a \log (F_j - \phi_j) + b$$

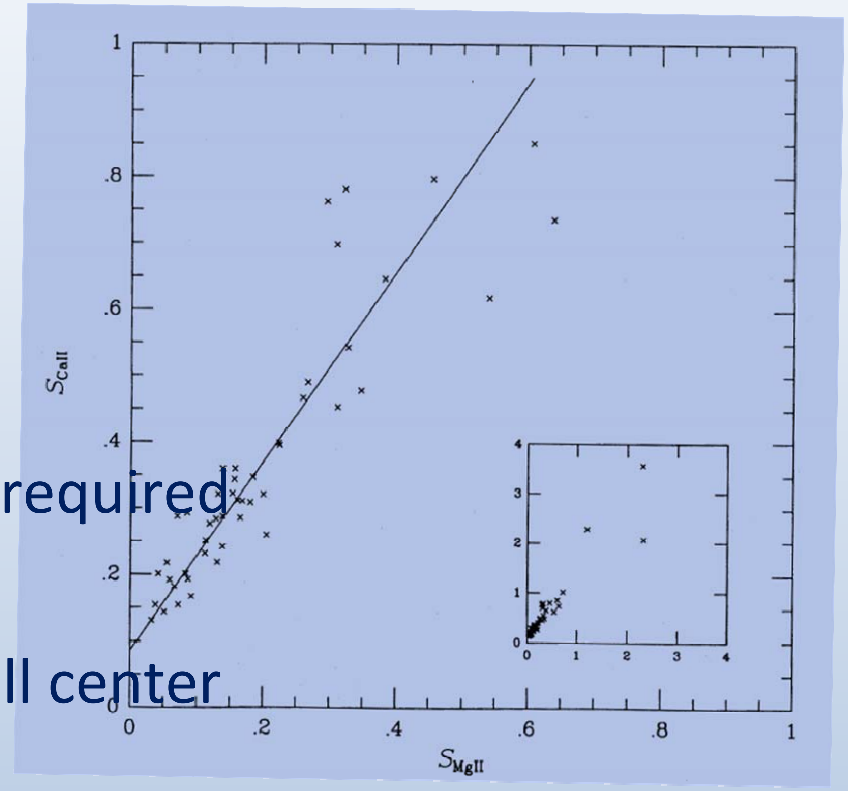

•Schrijver et al. (1987): **acoustic** origin

•Schrijver et al. (1989): basal chromosphere required

•Schrijver et al. (1992): basal flux

← supergranular cell center

•Judge et al. (2003): inter network fields: Lites (2002)

•Fossum & Carlsson (2006): × acoustic flux

•Jefferies et al. (2006): magneto-acousitic wave leakage ⇔ spicules

•Schrijver & Title (2003): magnetic carpet

Carbon Monoxide Thermal Profiling

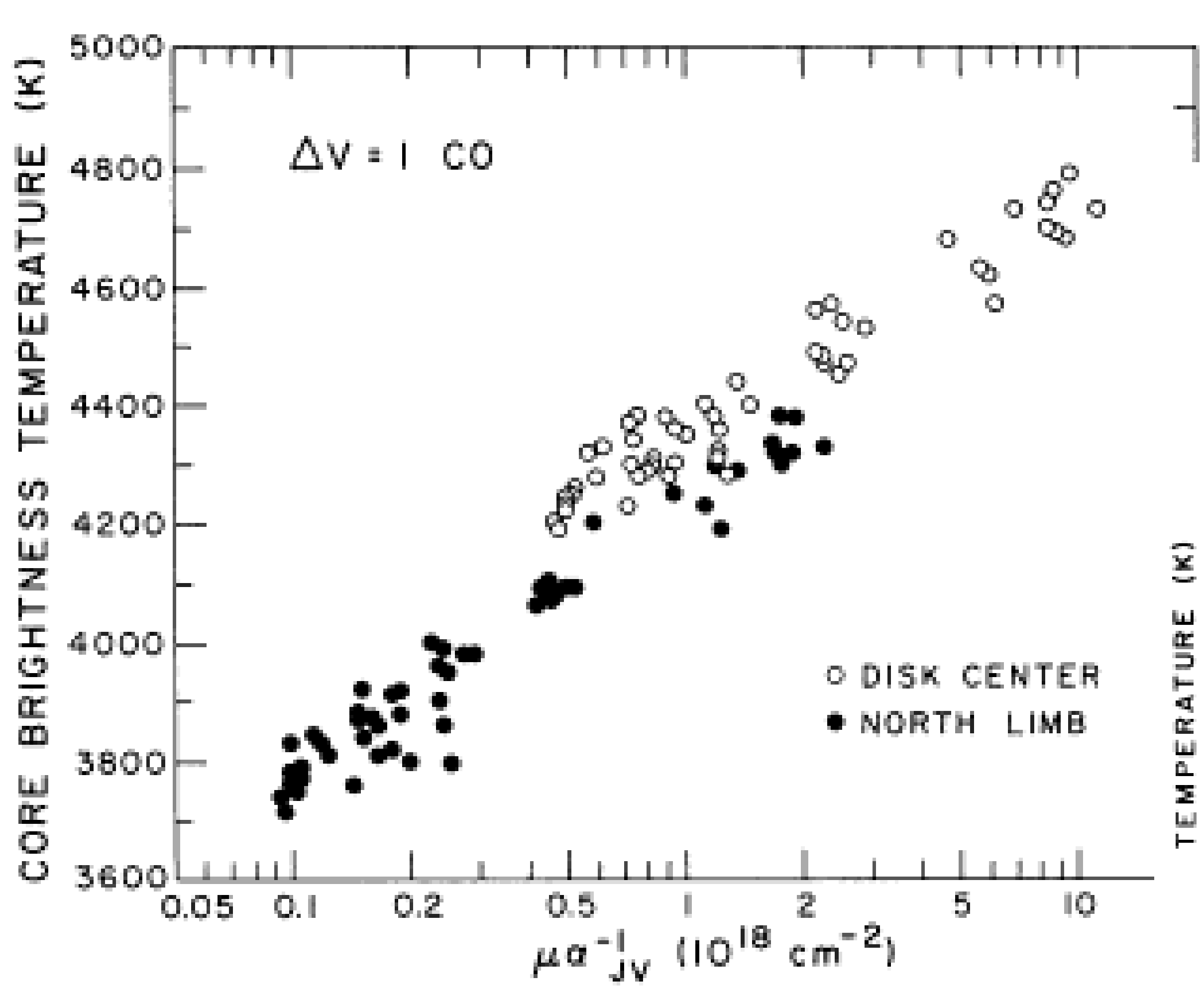

Ayres & Testerman (1980) ApJ 245, 1124

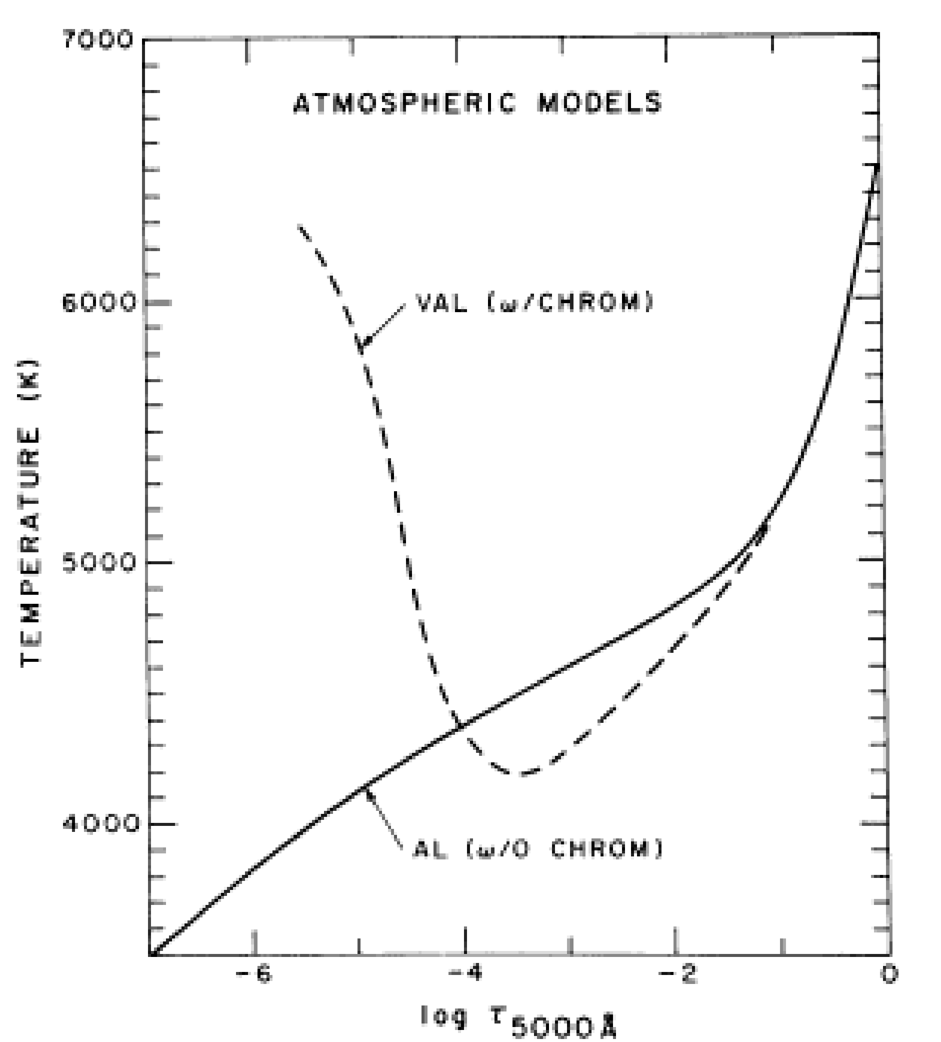

Carbon Monoxide Thermal Profiling

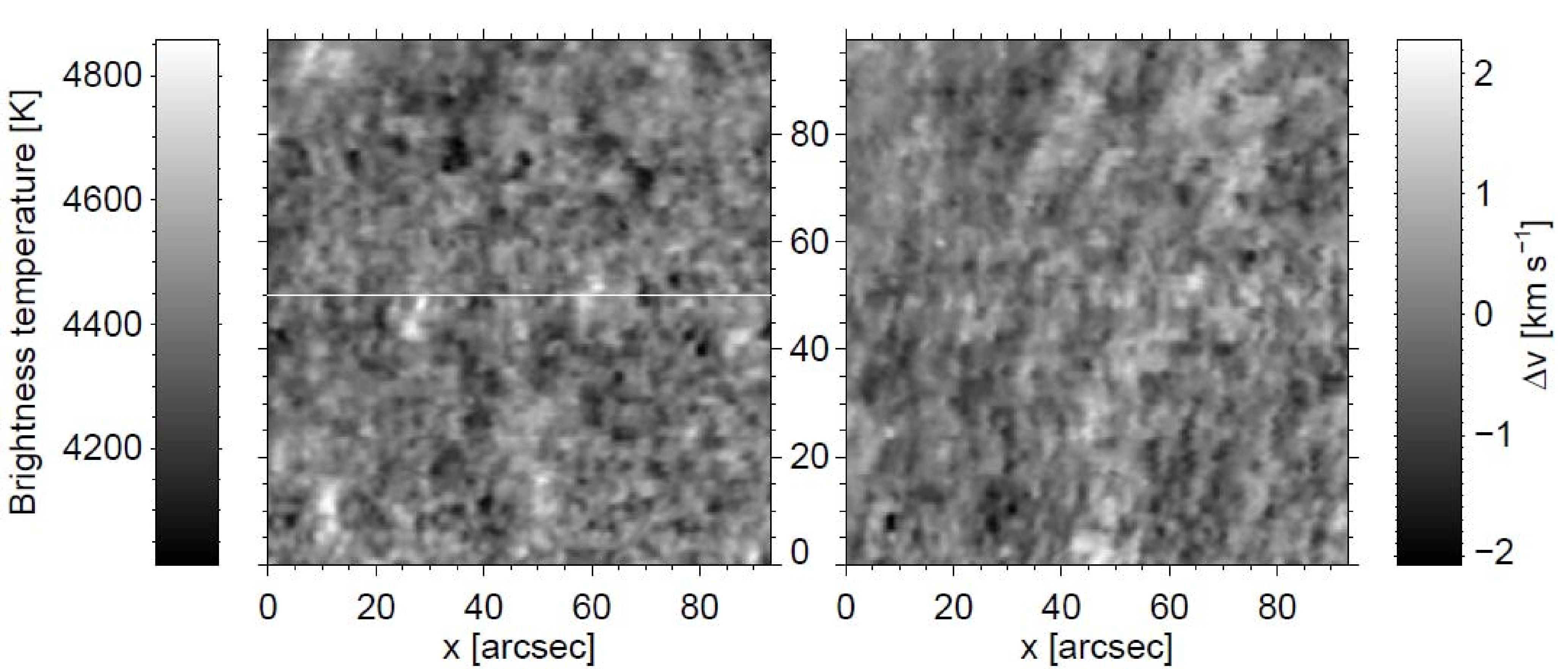

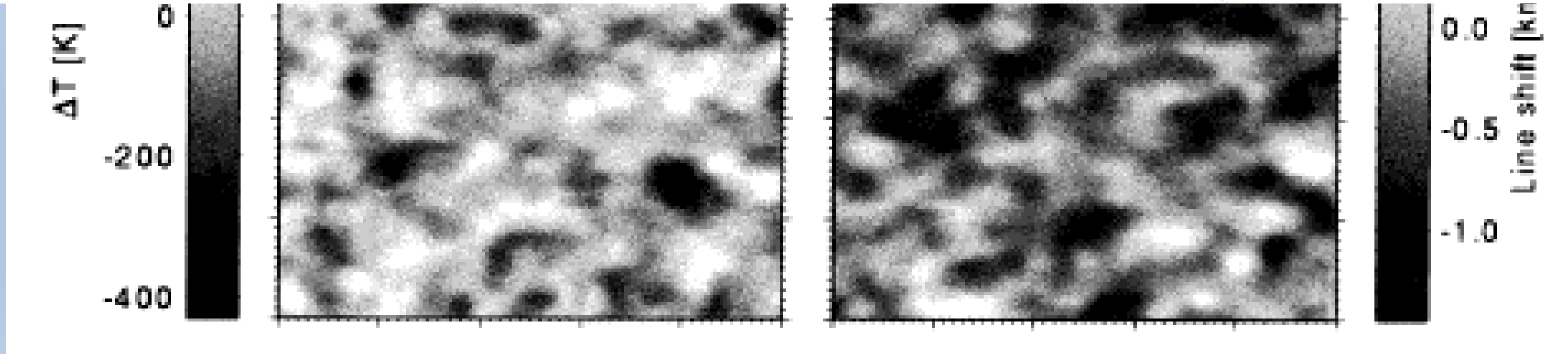

Uitenbroek, Noyes, Rabin: 1994, ApJ 432, L67.

Uitenbroek: 2000, ApJ, 531,571.

Carbon Monoxide Thermal Profiling

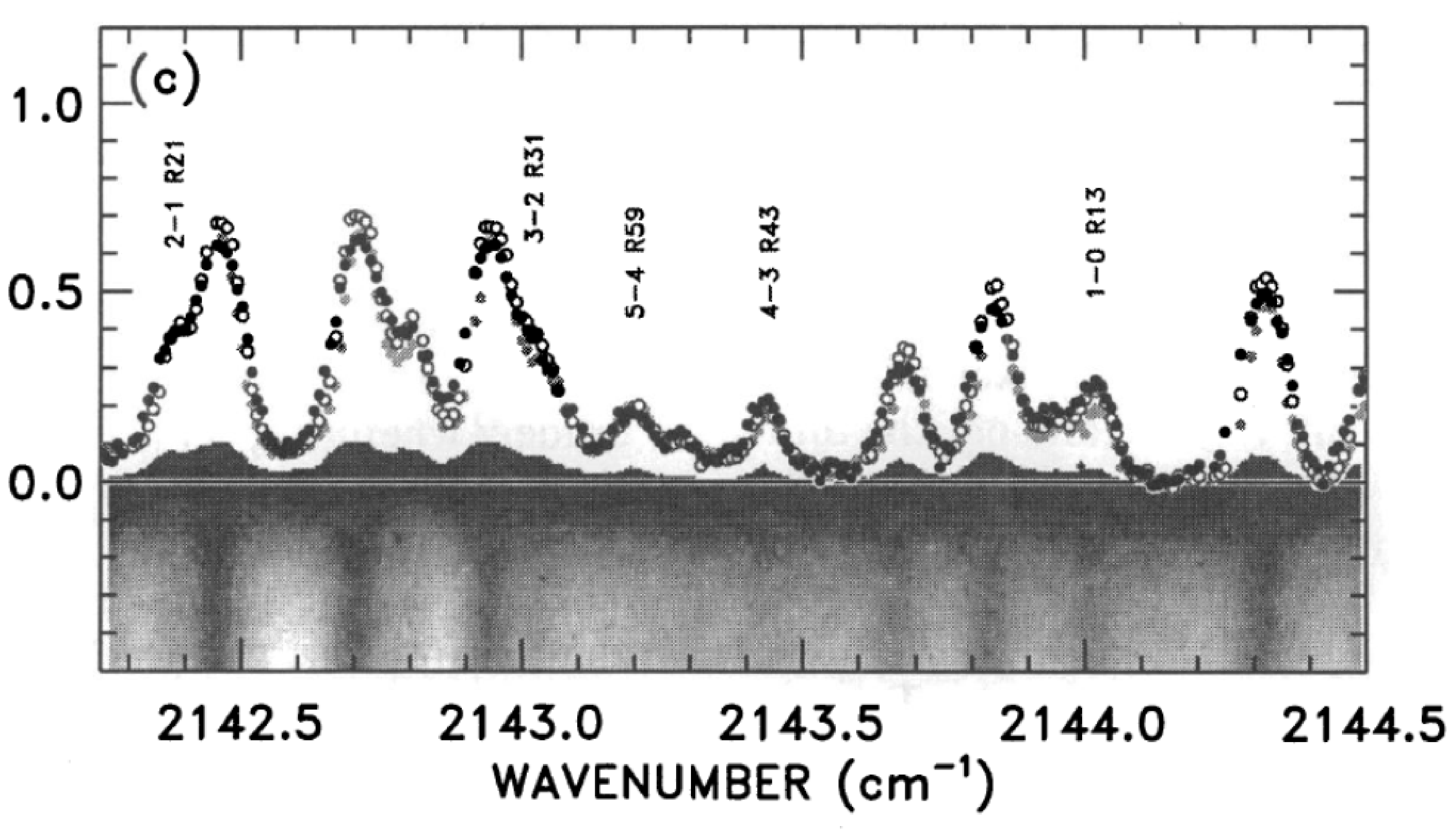

Ayres & Rabin (1996)

COmosphere

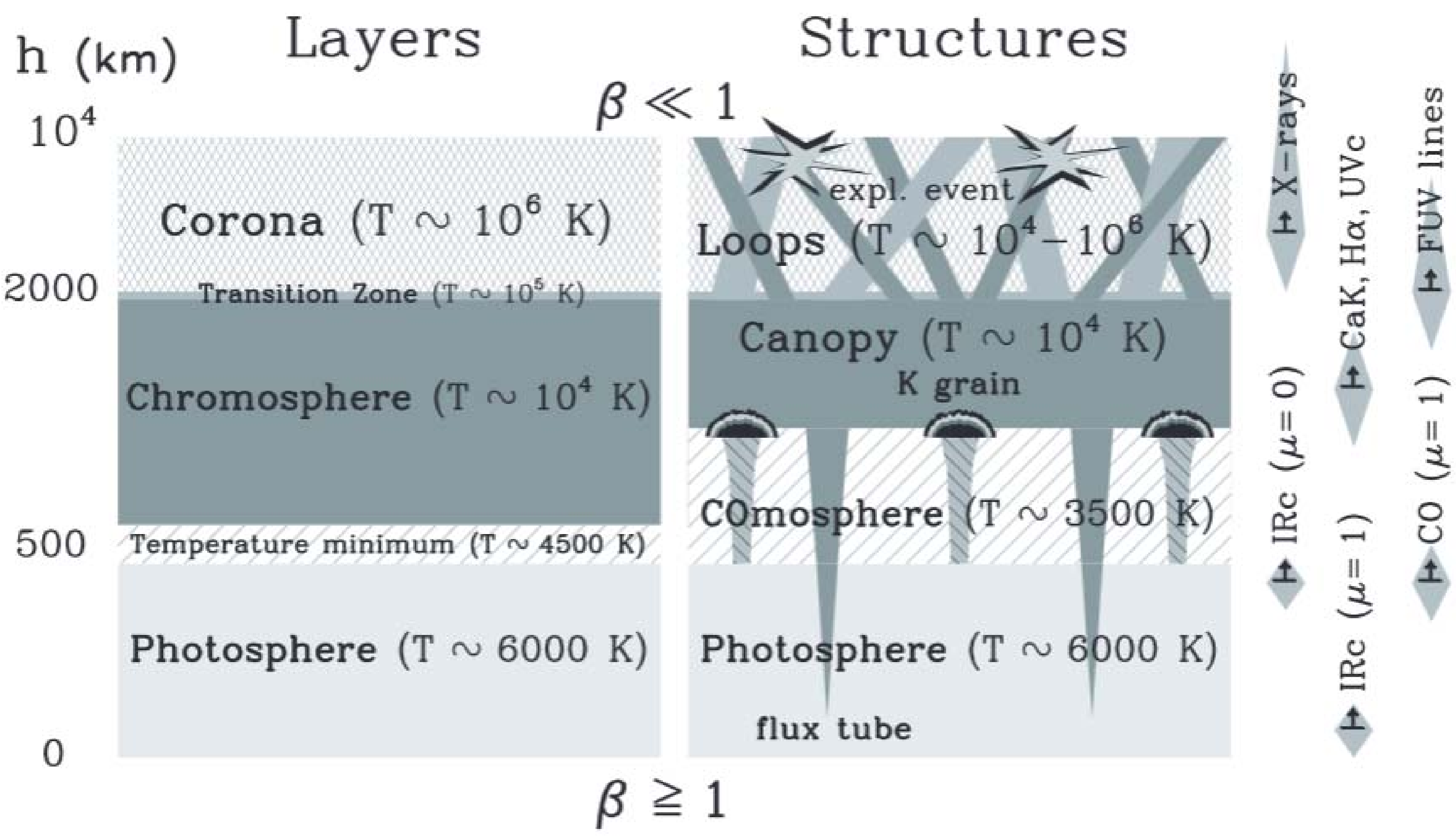

FIG. 1.—Two cartoons of outer solar atmosphere, encompassing alternative views of key "magnetic transition zone" (β is the ratio of gas to magnetic pressure). *Left*: Classical *layered* paradigm. *Right*: More modern *structured* picture (implicitly also time-dependent). Diamonds indicate approximate formation altitudes for different species, "UVc" is the far-UV (~1500 Å) continuum, "IRc" is the 4.7 μm thermal infrared continuum, $\mu = 1$ refers to disk center, and $\mu = 0$ is the extreme limb.

Thermal Bifurcation (Ayres 1981, ApJ 224,1064.)

coolant CO & heater/coolant H^-

$F = e_{co} + e_{H^-}$ (=0; radiative equilibrium)

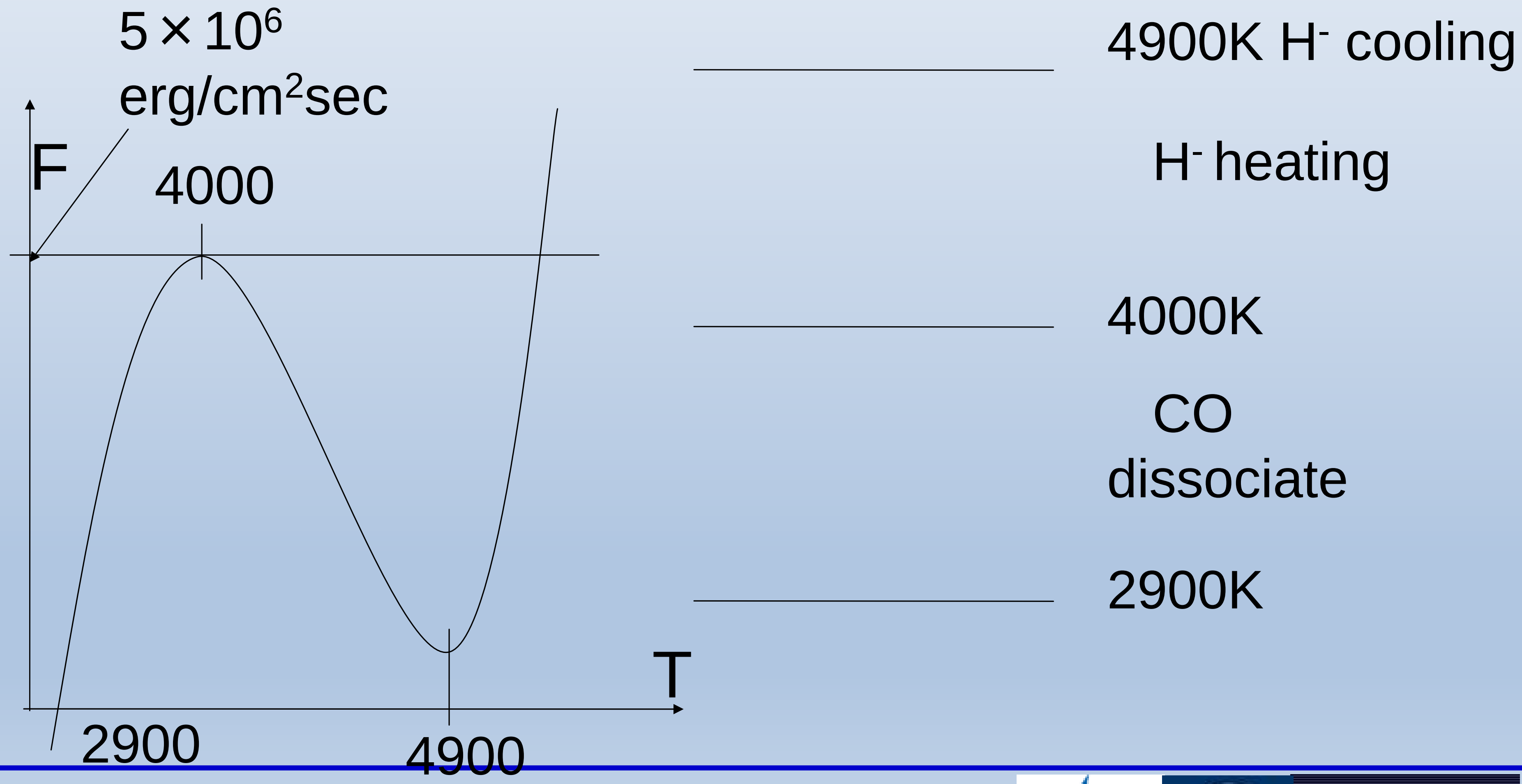

COmosphere

- Ayres (1981,...): CO - no temperature inversion
- Solanki et al. (1994): limb emission
- Uitenbroek et al. (1994): CO region punctuated by hotter region
- Ayres & Rabin (1996): 400 - 500 - 1,000 km above $\tau_{5000} = 1$
- ~ garanular sized region
- inter network

- Clark et al. (2004): dynamic: inverse Evershed flow
- × penumbral fibril pattern
- Pen & Schad (2012): highly sheared flows in the decay phase
- of a large flare (2011-02-17)

Conclusions

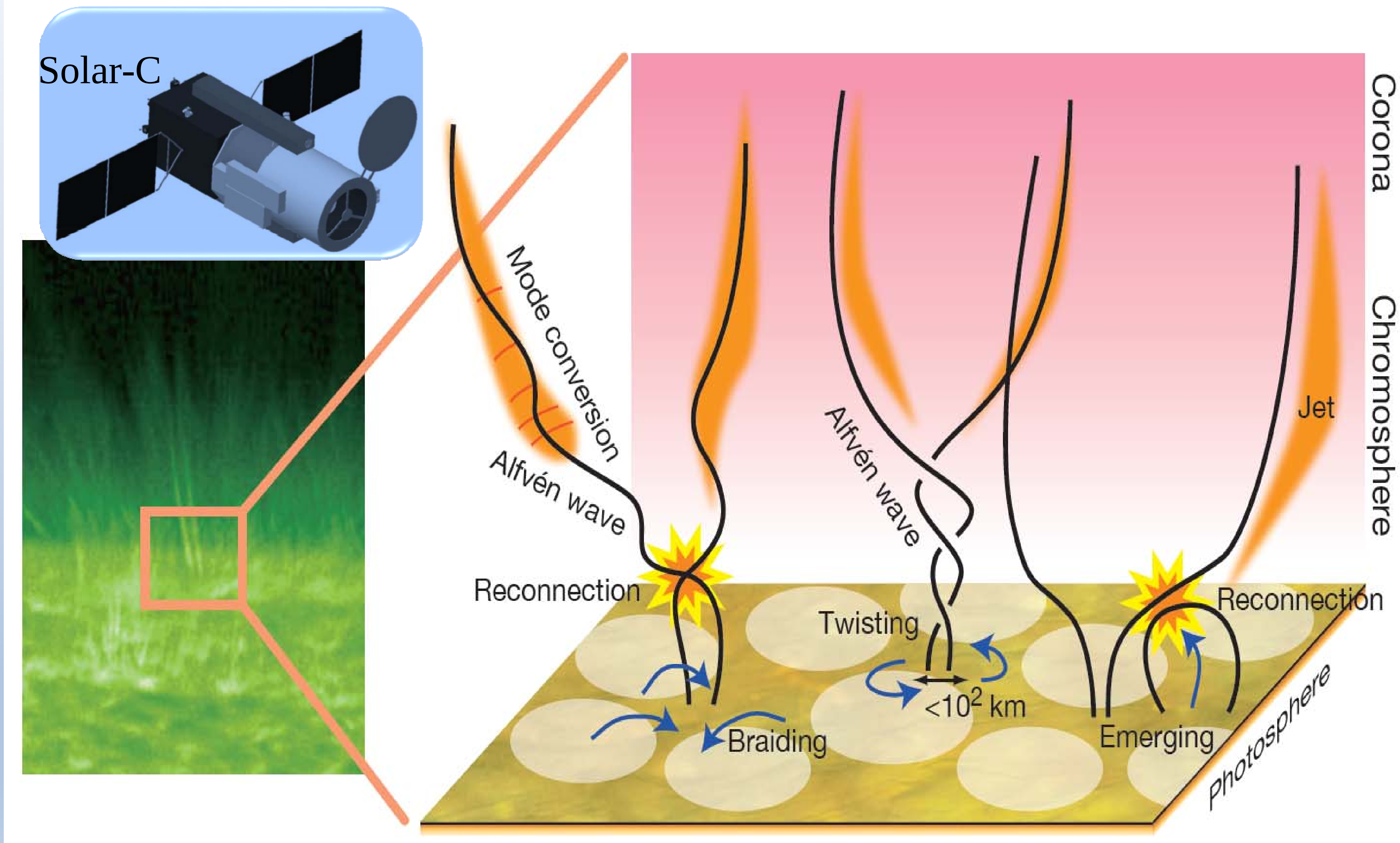

Solar-Cミッション提案書より